

## Forming of noncircular cross-section SiO<sub>2</sub> glass fibers

Markus Wegmann, Juliane Heiber, Frank Clemens and Thomas Graule

Eidgenössische Materialprüfungs- und Forschungsanstalt (EMPA), Dübendorf (Switzerland)

Dagmar Hülsenberg

Technische Universität Ilmenau, Ilmenau (Germany)

Kay Schuster

Institut für Physikalische Hochtechnologie (IPHT), Jena (Germany)

---

Silica glass fibers with triangular and rectangular cross-sections have been produced by two different means, namely preform drawing and powder extrusion. For the preform drawing method, silica glass rods were machined and polished to yield preforms with the desired cross-sections. These were then heated to temperatures in excess of 1600 °C and drawn to fibers with approximately 265 μm × 265 μm × 265 μm triangular and 275 μm × 100 μm rectangular cross-sections exhibiting tensile strengths between 300 and 400 MPa and bending radii smaller than 50 mm. For the extrusion route, a silica nanopowder was compounded at ≈150 °C with a polyethylene-based binder and extruded at similar temperatures through dies with the desired exit cross-section. The fibers were debound by thermally decomposing the binder and sintered at 1100 °C to yield amorphous glass fibers with approximately 205 μm × 205 μm × 205 μm triangular and 275 μm × 90 μm rectangular cross-sections. Although the two manufacturing processes are radically different, both involve flow of a fluid with a temperature-dependent viscosity and this dictates that shape trueness (i.e. flat faces and sharp corners) is a function of the drawing and extrusion rates and the temperature during drawing and sintering.

---

### 1. Introduction

Low thermal expansion and high thermal shock resistance, low electrical and thermal conductivity, high softening temperature, good optical transmission from ultraviolet through infrared wavelengths, and excellent resistance to chemical attack have made fused silica (SiO<sub>2</sub>) the material of choice for a wide variety of applications in the lighting, optical, chemical and semiconductor industries. Next to its use in the semiconductor industry as furnace furniture and crucibles for the processing of high-purity silicon, SiO<sub>2</sub> glass is used as a substrate material for electronic devices with processing temperatures in excess of 600 °C (i.e. vapor deposition methods). Such temperatures preclude the use of borosilicate and soda-lime-silica glasses whose components may diffuse into and poison electronically active surface layers.

On this basis, fused SiO<sub>2</sub> in fiber form is a candidate substrate material for research efforts currently being made to integrate digital processing power into textile materials by applying electronic circuitry directly onto fibers in a fabric [1]. For the development of a fiber-based computer, it must be considered that integrated circuit fabrication methods depend not only on high temperatures, but also on radi-

ation and subatomic particles being focused on the substrate and circuit surfaces during various etching and deposition processes. Fibers with a circular cross-section do not possess a flat plane on which such beams can be focused, and therefore the need for a fiber with at least one flat face is generated.

Regarding silica, several methods are available for producing the material in fiber form, including fiber melt spinning, preform drawing and sol-gel processing [2]. For high-purity silica, the melting approach is handicapped by processing temperatures in excess of 2000 °C, which can promote the absorption of impurities by the melt from the glass melting apparatus (walls, heating elements, tools) [3]. With reference specifically to producing fibers with noncircular cross-sections, the low viscosity needed to spin the fibers makes retention of a noncircular cross-section after passing the melt through a shaped orifice (nozzle) highly problematical.

Maintaining purity in the preform drawing process is not such a big problem. With exception of the two preform ends, the primarily vapor-deposited preforms manufactured from high-purity precursors do not come into contact with the processing apparatus. Furthermore, relative to the melting process, the viscosity during drawing is significantly higher due to lower processing temperatures on the order of 1600 °C, and this should permit free-standing shaped pre-

---

Received 18 October 2004, revised manuscript 3 February 2005.

forms to be drawn into profile fibers with the same cross-sections in miniature without significant rounding of flat faces and sharp edges. Drawing of fibers with complex cross-sections has previously been achieved by embedding shaped preforms in a glass cladding of different composition with a circular cross-section prior to drawing and etching away the cladding from the fiber after drawing [4].

Significantly lower process temperatures than for either melting or drawing are required to produce glass fibers by the sol-gel route. A chemically-prepared gel is drawn down into a fiber and the dried precursor fiber is subsequently densified at temperatures around 1200 °C [5 and 6]. High-purity bulk SiO<sub>2</sub> has been prepared by this method [7], but with regards to forming shaped fibers, this method is handicapped by high sintering shrinkage and workpiece distortion due to the low achievable densities in the dried gels.

In addition to the processing routes just described, powder extrusion has also been used to produce long shapes of SiO<sub>2</sub> glass. Here, a high-purity silica powder is mixed with polymeric binder and the resulting mixture extruded through dies which impart the desired cross-section and size on the extrudate. The binder is subsequently removed from the extrudate (debinding) and the silica powder is sintered at temperatures around 1200 °C. This method was pioneered by Clasen using aqueous-based binders to produce bulk SiO<sub>2</sub> [8 and 9] and has recently been used with a thermoplastic binder to prepare silica fibers with circular cross-section [10]. While thermoplastic binders are more difficult to debind after extrusion than aqueous-based binders, they are much less prone to phase separate from the inorganic powder under pressure during extrusion. Furthermore, shape retention after extrusion is generally better for thermoplastic-based extrudates than for extrudates produced using water-based binders.

In the work described below, the preform drawing method and the powder extrusion method with a thermoplastic binder were used to fabricate SiO<sub>2</sub> glass fibers with rectangular and triangular cross-sections with dimensions to suit the needs of the proposed application of the fibers as substrates for a fiber-based computer.

## 2. Experimental procedure

### 2.1 Drawing

High-purity synthetic SiO<sub>2</sub> rods 300 mm long of 22 mm diameter circular cross-section (Suprasil series; Heraeus, Hanau (Germany)) were used as the starting material for the fiber drawing process. The rods were machined and polished to an optical-quality finish with either an equilateral triangular cross-section with a 17 mm edge, or to a rectangular cross-section with edges 18.5 mm × 6.5 mm. A given preform was then suspended from a load cell attached to a cross-head positioned over a vertical tube furnace (Thermal Technology GmbH, Bayreuth (Germany) and subsequently passed through the argon-filled furnace hot zone by lowering the cross-head at a controlled rate (preform feed rate). Underneath the furnace, the softened glass was drawn off as a fiber at a controlled rate (fiber drawing rate) via a capstan and finally wound onto a drum.

The desired fiber cross-sectional dimensions were fixed at a 260 μm edge for the equilateral triangle and 283 μm ×

100 μm for the rectangle. Based on the dimensions of the respective preforms, the desired draw-down ratios ( $V$ ) could be calculated according to

$$V = \left( \frac{a_p}{a_f} \right)^2 \quad (1)$$

where  $a_p$  and  $a_f$  are the radii of the preform and the desired fiber, respectively, approximated by the radii of the circles which circumscribe the given cross-sections [11]. For a given preform feed rate ( $v_p$ ), the fiber drawing rate ( $v_f$ ) which would yield a fiber with the desired dimensions could then be calculated according to

$$v_f = V \cdot v_p \quad (2)$$

At a 1.0 mm/min preform feed rate, triangular and rectangular fibers were thus drawn at rates of 4.22 and 4.17 m/min, respectively. Rectangular fibers were also drawn at 8.34 and 12.52 m/min with preform feed rates of 2.0 and 3.0 mm/min, respectively.

The furnace temperature was controlled between 1850 and 1950 °C via a pyrometer aimed at the surface of the graphite tube surrounding the hot zone. The temperature of the preform in the draw-down region, which is different from that of the surrounding furnace tube due to heat being lost to the preform outside the hot zone and to the argon gas flow, was determined indirectly from other process parameters via the viscosity of the glass in the draw-down region. The viscosity ( $\eta$ ) was determined using the equation

$$\eta = \frac{F}{6 \pi a_p^2 v_p \ln \left( \frac{a_p}{a_f} \right)} z_b \quad (3)$$

where  $F$  is the tensile force on the fiber resulting from the capstan pulling on the fiber,  $z_b$  is the axial length of the draw-down region, and the remaining parameters are as defined above [12]. The tensile force was calculated from the force on the load cell from which the preforms were suspended. The force measured by the load cell was a combination of the force of the capstan pulling on the fiber and the force of gravity acting on the preform, and in order to obtain  $F$  above, the force of gravity had to be subtracted from the measured value while taking into account the constant gradual decrease in the mass of the preform as the fiber is pulled off.

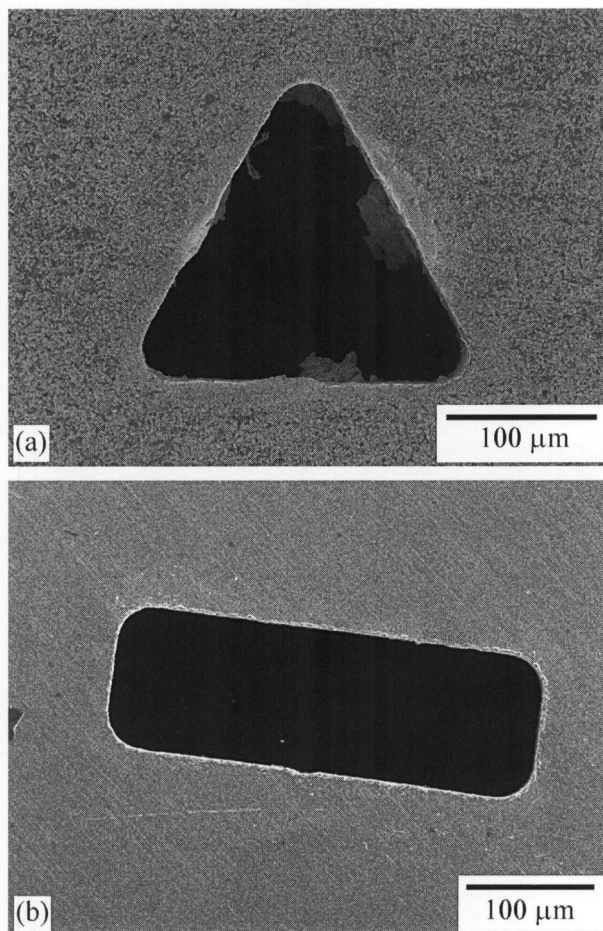
With the viscosity having been calculated, the temperature  $T$  of the draw-down region could be determined using the Vogel-Fulcher-Tammann equation

$$T = \frac{B}{\lg \eta - A} + C \quad (4)$$

where  $A$ ,  $B$  and  $C$  are constants. These constants for the silica glass used here were calculated from the reference temperature and viscosity data provided by the preform supplier for the softening, annealing, and strain points ( $\eta = 10^{6.6}$ ,  $10^{12}$  and  $10^{13.5}$  Pa s, respectively).

### 2.2 Extrusion

Using the work of Clasen [8] for reference, nanosized fumed silica powder Aerosil OX 50 (Degussa (Schweiz) AG, Baar



Figures 1a and b. SEM pictures of orifice profiles of fiber extrusion dies; a) triangular, 260  $\mu\text{m}$  edge, and b) rectangular, 115  $\mu\text{m}$   $\times$  350  $\mu\text{m}$  edges (dimensions measured as the distance between the intersections of the tangents to the faces). The surface irregularities visible inside the triangular die are feedstock residues left over from an extrusion trial.

(Switzerland)) with a specific surface area of 55 m<sup>2</sup>/g was used to prepare extrusion feedstocks. The powder characteristics have been presented in detail elsewhere [10].

The silica powder (40 to 48 vol.%) was blended with the binder in an electrically-heated twin-blade (Banbury) mixer driven by a torque rheometer (Haake Rheomix 3000 and Rheocord 9000, respectively; Thermo Electron Corp., Speyer (Germany)). The thermoplastic binder system used was a 9:1 by volume mixture of low-density polyethylene (LDPE; Lacqtene series, Elf Atochem, Puteaux (France)) and wax (Licomont EK series, Clariant GmbH, Augsburg (Germany)) [10]. Mixing was performed at 150°C for 180 min. At the end of the 3 h of mixing, the measured torque had generally reached a constant value and this was taken as an indication that the process of distributing the powder homogeneously in the binder was complete.

After compounding, the feedstocks were extruded vertically downwards using a capillary rheometer (Rosand RH7-2, Malvern Instruments Ltd., Malvern (UK)) with a 24 mm diameter barrel at temperatures between 140 and 220°C through dies with the exit cross-sections shown in figures 1a and b. For both cross-sections, dies of two different lengths were used. These were characterized by the ratios  $L/D_{\text{eq}} =$

0.17 and 1.7, where  $L$  is the length of the die land and  $D_{\text{eq}}$  is the diameter of the circle which circumscribes the given cross-section. The rate of extrusion was controlled by varying the rate of travel of the ram ( $v_r$ ) in the barrel between 0.7 and 2.7 mm/min.

Extrudates were cut into 10 cm lengths and thermally debound in air by ramping at 15 K/h up to 500°C and holding 2 h, then continuing at 150 K/h up to 750°C and holding a further 2 h. Fibers were sintered under air on Al<sub>2</sub>O<sub>3</sub> substrates by ramping at 15 K/h to 1100°C and holding for 4 h.

### 2.3 Analyses

At the various stages of processing described above, samples were characterized using scanning electron microscopy (SEM, Vega TS 5130, TeScan s.r.o., Brno (Czech Republic)), X-ray diffraction (XRD; Model D-500, Siemens AG, Munich (Germany)) and thermal gravimetric analysis (TGA; Netzsch STA 409, Netzsch Gerätebau GmbH, Selb (Germany)).

Tensile strength measurements on fibers were performed on samples with a free clamping length of 50 mm at a cross-head velocity of 0.3 mm/min (Model Z005 Universal Testing Machine, Zwick Testing Machines Ltd, Leominster (UK)). The procedure for mounting the fibers in preparation for tensile testing is described in detail elsewhere [13].

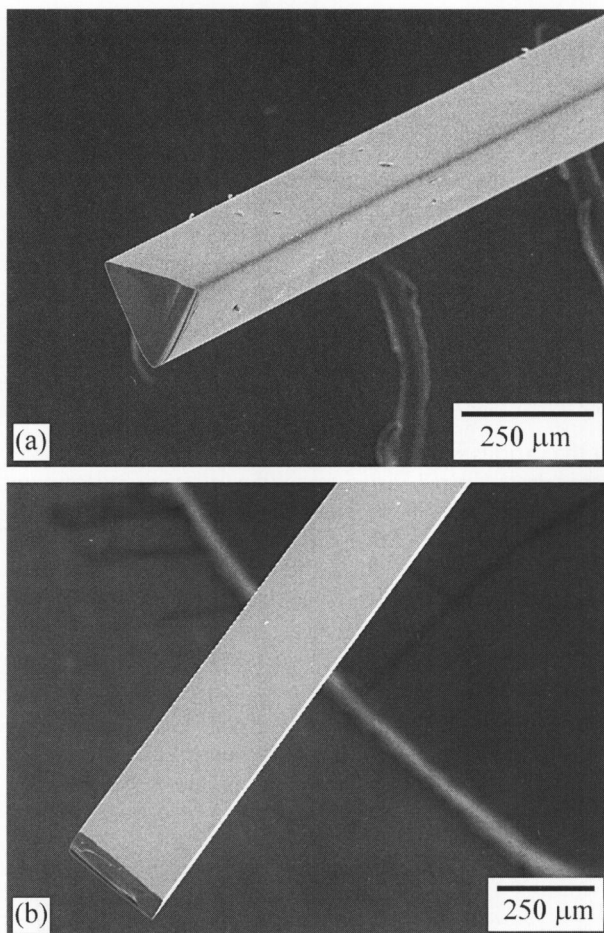
## 3. Results and discussion

### 3.1 Drawing

Profile fibers several hundred meters long of both geometries were obtained without breakage using the drawing process. SEM images of samples of the drawn fibers are shown in figures 2a and b. As noted above, the targets for the fiber cross-sectional dimensions were 260  $\mu\text{m}$  edges for the equilateral triangle and 283  $\mu\text{m}$   $\times$  100  $\mu\text{m}$  for the rectangle. Measurements on fibers drawn at the 1900°C pyrometer setpoint showed that the true dimensions agreed very well with these calculated values, with 265  $\mu\text{m}$  edges being obtained for the former and 275  $\mu\text{m}$   $\times$  100  $\mu\text{m}$  for the latter.

The effect of temperature on the drawing process at a fixed preform feed rate of 1.0 mm/min and drawing rates of 4.22 and 4.17 m/min for the triangular and rectangular cross-sections, respectively, was investigated by drawing fibers at pyrometer-controlled setpoints of 1850, 1900 and 1950°C. The corresponding calculated glass viscosities and glass temperatures are summarized in table 1. At the 1850°C setpoint, no data could be collected for the rectangular cross-section since the glass viscosity was too high for drawing and the fiber broke repeatedly. The triangular fiber also exhibited a tendency to break at this temperature, however, sufficient data could be collected to perform the analysis. The results show that the glass temperature in the draw-down region was always about 200°C lower than the temperature measured by the pyrometer.

Figures 3a and b show that with increasing temperature and corresponding decreasing viscosity, the corners of the

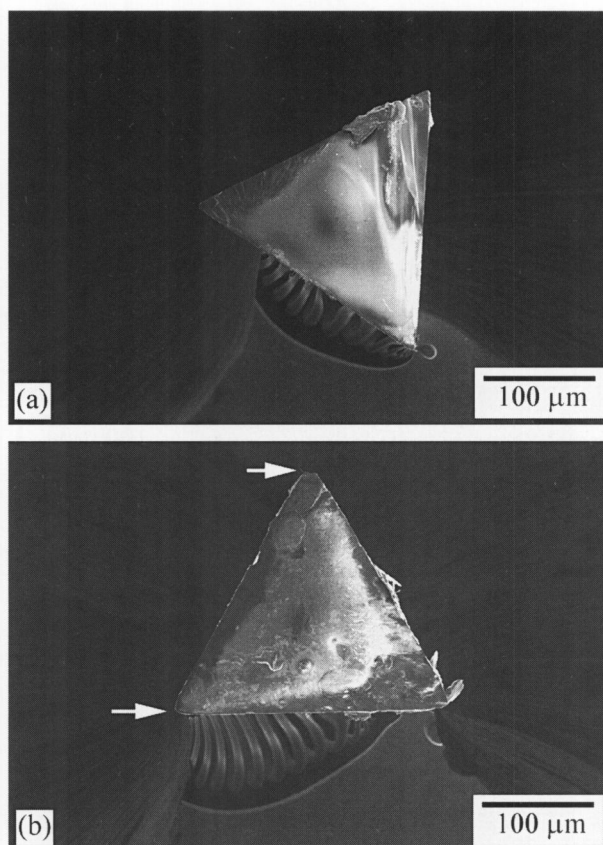


Figures 2a and b. SEM pictures of drawn fibers; a) 1900°C at a 4.22 m/min drawing rate, and b) 1900°C at a 4.17 m/min drawing rate, both with a preform feed rate of 1.0 mm/min.

Table 1. Fiber drawing parameters for a 1.0 mm/min preform feed rate

	triangular		rectangular	
	glass temperature in °C	lg $\eta$ in Pa s	glass temperature in °C	lg $\eta$ in Pa s
pyrometer setpoint temperature in °C				
1850	1650	6.20	—	—
1900	1691	5.84	1682	5.93
1950	1747	5.43	1731	5.55

profiles become blunter. As the viscosity decreases, surface tension forces are sufficient to cause rounding off of the edges while the fiber is in the furnace hot zone. This effect at the higher drawing temperatures can be countered by increasing the drawing rate (and the preform feed rate accordingly): rectangular fibers drawn at 12.52 m/min at the 1900°C setpoint exhibited edge definition as good as that observed for fibers drawn at 4.17 m/min at the 1850°C setpoint (analogous conditions to figure 3a). At the higher drawing rate the fiber has a shorter residence time in the furnace hot zone and the glass has less time to flow axially under the influence of surface tension, thereby preventing rounding from occurring.



Figures 3a and b. SEM pictures of fracture surfaces of fibers drawn at a) 1850°C, and b) 1900°C, both with a 4.22 m/min fiber drawing rate. White arrows point to locations where rounding is observed.

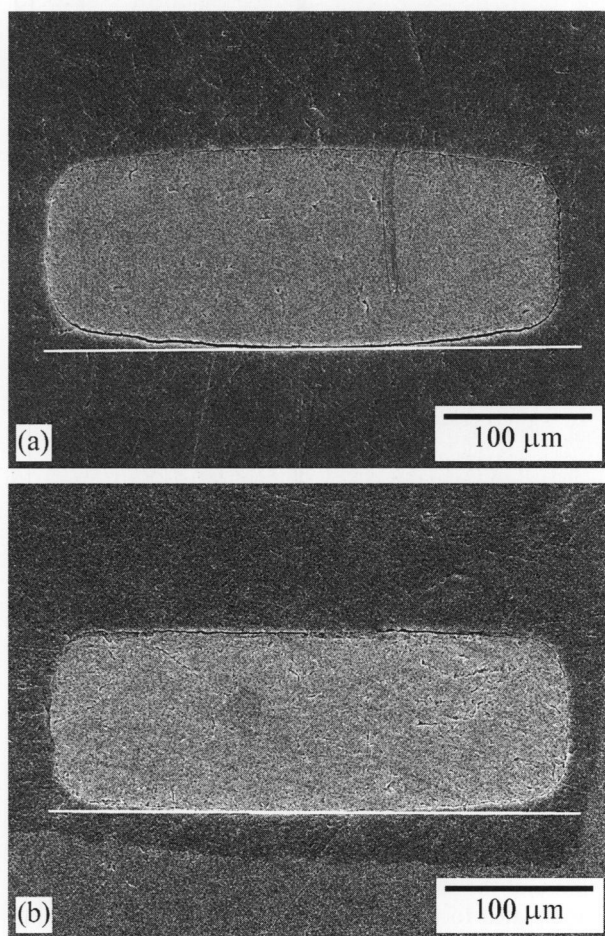
The drawn fibers all exhibited bending radii better than 50 mm, and radii down to 10 mm were achieved in several cases. Tensile testing revealed average strengths on the order of 300 to 400 MPa. This is about three times higher than measured for bulk silica glass using standard testing methods, and corresponds with the experience that the strength of glasses and ceramics increases with decreasing part size. The strength data, shown summarized in table 2, showed no trends regarding strength and drawing temperature and strength and fiber cross-section. The relatively low calculated Weibull moduli are indicative of considerable scatter in the strength data. SEM investigation of the fracture origins after testing revealed that in general, fibers with low strengths were characterized by defects in the bulk, fibers with medium strengths by surface defects, and fibers with high strengths by defects along the fiber edges.

### 3.2 Extrusion

A number of processing parameters ( $L/D_{eq}$ , extrusion rate, extrusion temperature, solids loading) were varied to study their effect on the shape retention of the extruded cross-sections imposed by the dies shown in figures 1a and b. The effect of die length is apparent in figures 4a and b which shows cross-sections of green rectangular fibers with 40 vol.% loading which were extruded at 140°C and ram rate  $v_r = 0.7$  mm/min. Fibers extruded from the short die ( $L/D_{eq} = 0.17$ ; figure 4a) exhibit clearly more bowed faces

Table 2. Summary of tensile test results; 30 samples per set, CL = confidence limit on  $\sigma_{avg}$ 

pyrometer setpoint temperature in °C	triangular			rectangular		
	$\sigma_{avg}$ in MPa	90 % CL on $\sigma_{avg}$ in MPa	Weibull modulus	$\sigma_{avg}$ in MPa	90 % CL on $\sigma_{avg}$ in MPa	Weibull modulus
		(lower/upper)			(lower/upper)	
1900	380	345 / 419	3.3	315	292 / 338	4.4
1950	352	328 / 375	4.5	373	346 / 400	4.4



Figures 4a and b. SEM pictures of cross-sections of green fibers with 40 vol.% loading extruded at 140°C and a ram rate  $v_r = 0.7$  mm/min; a) die length-to-diameter ratio  $L/D_{eq} = 0.17$ , and b)  $L/D_{eq} = 1.7$ . White lines are provided as a guide to the eye to show rounding effects.

than fibers extruded from the long die ( $L/D_{eq} = 1.7$ ; figure 4b) at the same extrusion rate and temperature. A longer die land equates to a longer residence time of the feedstock in the die land at a given rate of extrusion, and this residence time increase allows the polymer in the material to relax more and reduce elastic springback (die swell) when the fiber leaves the die.

Conversely, by decreasing the residence time in the die by increasing the extrusion rate at constant temperature and die length, the time for the polymer molecules to relax in the die land is reduced and die swell is consequently promoted. Thus, at  $v_r = 2.7$  mm/min, rounded profiles similar to the one shown in figure 4a were produced using the long

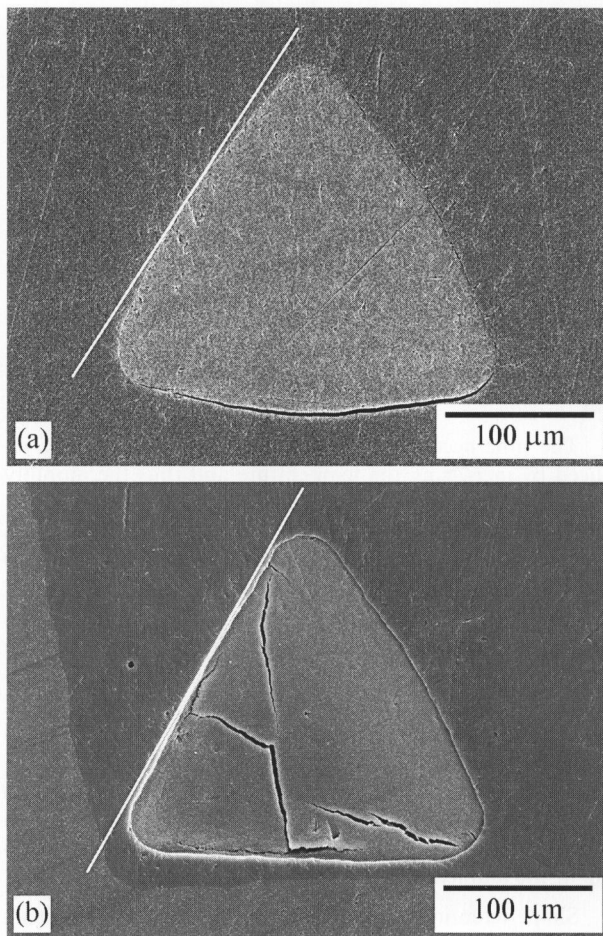
die which had resulted in the extrusion of fibers relatively flat faces at  $v_r = 0.7$  mm/min (figure 4b).

The time necessary for the polymer to relax can be reduced by increasing the temperature and thus the mobility of the polymer molecules, therefore it might be expected that fibers with flatter faces should result at higher extrusion temperatures. However, increasing the temperature from 140 to 220°C at constant die length and extrusion rate resulted in more pronounced curvature of the fiber faces at the higher temperature. The increased molecular mobility at the elevated temperature not only accelerates the relaxation process, it also greatly decreases the viscosity of the feedstock and this allows surface tension to pull the fiber faces into curves in order to minimize the surface energy of the system. The lower viscosity at the elevated temperature also resulted in the drawing down of the fibers under their own weight upon leaving the die and before solidifying by cooling in the ambient air.

Shape retention could clearly be improved by increasing the volume fraction of powder in the feedstock. This result shows well in figures 5a and b which depicts fibers of 40 and 48 vol.% solids loading extruded under otherwise identical conditions. On the one hand, reducing the binder phase fraction reduces the amount of elastic energy which can be stored by the feedstock during extrusion. Furthermore, the closer packing of high surface area powder particles results in greater interparticle friction in the feedstock. Both of these factors combine to reduce the propensity for the extrudates to change shape from the extruded profile under the influence of internal stresses, surface tension and gravity.

While shape retention is improved by the higher solids loading, the mechanical integrity of the green fibers is reduced because the polymer matrix becomes increasingly discontinuous. This is manifested by a reduction in tensile strength of the green fibers from  $(17.9 \pm 0.8)$  to  $(12.3 \pm 1.0)$  MPa. The tears in the polished cross-section in figure 5b are also a consequence of the higher loading which leads to the green fibers becoming increasingly brittle. These defects are artifacts from the polishing procedure where the lateral forces during grinding and polishing on the exposed face cause the material to fracture.

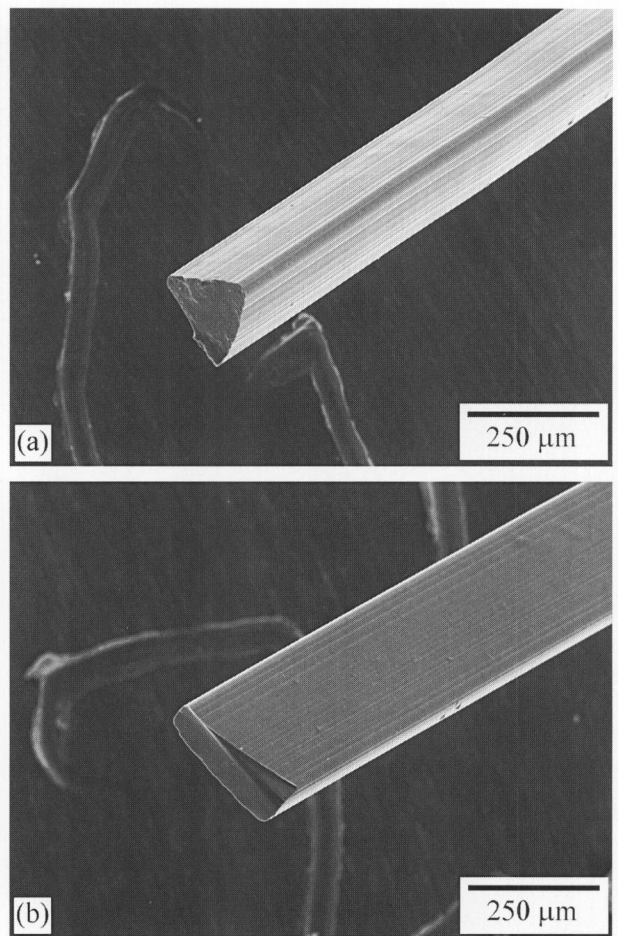
Green fibers up to 125 m in length could be extruded. The extrusion of longer fibers was precluded by the presence of agglomerates in the feedstocks which would block the dies. In general, the rectangular cross-section dies were more likely to become blocked than those with the triangular cross-section. It is assumed that while in the triangular dies agglomerates can move to the center of the die land where its height is 200  $\mu$ m, the rectangular dies have a maximum die land height of only 115  $\mu$ m, thereby making the rectangular dies more susceptible to blockages.



Figures 5a and b. SEM pictures of cross-sections of green fibers extruded at 140 °C with a ram rate  $v_r = 2.0$  mm/min and die length-to-diameter ratio  $L/D_{eq} = 0.17$ ; a) 40 vol.% loading, and b) 48 vol.% loading. White lines are provided as a guide to the eye to show rounding effects.

SEM images of sintered amorphous fibers are shown in figures 6a and b. In the 48 vol.% case, the sintered fiber dimensions were on the order of  $205 \mu\text{m} \times 205 \mu\text{m} \times 205 \mu\text{m}$  edge for the triangular and  $275 \mu\text{m} \times 90 \mu\text{m}$  for the rectangular cross-sections. Relative to the dimensions of the green fibers, the 40 vol.% fibers experienced on the order of 26.1 % linear shrinkage, the 48 vol.% fibers 21.6 % during sintering. The theoretically possible linear shrinkage in the former case is 26.3 %, in the latter 21.7 %, indicating that close to 100 % densification was achieved in both cases. XRD analysis confirmed that the sintered material is amorphous.

The fibers invariably became warped during sintering and this made tensile testing of sintered fibers impossible since no perfectly straight lengths of material could be obtained. Work is continuing to increase the powder loading and thereby decrease the magnitude of the shrinkage which will help to reduce the amount of distortion during sintering. Due to the presence of the spatially localized defects which are visible on the faces of the fibers in figures 6a and b, the strength of the extruded and sintered fibers is expected to be lower than that of the drawn fibers. The defects are assumed to stem from the powder agglomerates already referred to above which were not destroyed during the feed-stock mixing process.



Figures 6a and b. SEM pictures of sintered fibers; a) 48 vol.% loading, 140 °C,  $v_r = 2.0$  mm/min,  $L/D_{eq} = 0.17$ , and b) 40 vol.% loading, 140 °C,  $v_r = 2.7$  mm/min,  $L/D_{eq} = 1.7$ .

Comparing figures 2a and b, and 6a and b, it is clear that the edges of the extruded and sintered fibers are not as sharp as those of the drawn fibers and that the extruded fibers exhibit a surface texture aligned parallel to the fiber axis. Reference to figures 1a and b shows that the edge definition and the surface quality of the sintered fibers are directly related to the quality of the dies used for extrusion. Both factors are limited by the laser machining process used for cutting the dies, the former by a finite cutting radius of the laser beam and the latter probably by mechanical vibrations in the equipment and the workpiece. It is possible that the mechanically prepared  $\text{SiO}_2$  glass preforms have edges and surface texture of similar absolute dimensions, however, since these are reduced in size during drawing by a factor of  $22 / 0.25$  (preform edge length / fiber edge length) = 88, the edges of the drawn fibers are sharper and the surface quality better than in the extruded case. Furthermore, preform surface irregularities will also be smoothed out by surface tension effects at the high temperatures experienced during drawing.

#### 4. Summary and conclusions

Silica glass fibers with triangular and rectangular cross-sections have been produced by  $\text{SiO}_2$  glass preform drawing as well as by  $\text{SiO}_2$  powder extrusion and sintering. For the

preform drawing method, 22 mm diameter amorphous silica glass rods were machined and polished to yield preforms with the desired cross-sections. These were heated to temperatures in excess of 1600 °C and drawn to fibers with approximately 265 μm × 265 μm × 265 μm triangular and 275 μm × 100 μm rectangular cross-sections. Rounding of the fiber edges could be reduced by drawing at high viscosities and high drawing rates, thereby countering the effect of surface tension. The fibers exhibit high tensile strengths on the order of 300 to 400 MPa. Bending radii smaller than 50 mm and down to 10 mm were achieved. Thus, this study has shown that high-quality continuous SiO<sub>2</sub> glass fibers with well-defined noncircular profiles can be produced using the preform drawing method.

For the extrusion route, between 40 and 48 vol.% silica nanopowder with a specific surface area of 55 m<sup>2</sup>/g was compounded at 150 °C with a polyethylene/wax binder. Feedstocks were subsequently ram-extruded at temperatures between 140 and 220 °C through dies with the desired exit cross-sections. Rounding of the faces and edges of the extrudates could be reduced by using dies with long die lands, and by extruding at low temperatures and high rates. Shape retention was also improved by increasing the solids loading from 40 to 48 vol.%. The binder was removed from the green fibers by thermal decomposition in air. The debound articles were sintered at 1100 °C in air to yield amorphous fibers with approximately 205 μm × 205 μm × 205 μm triangular and 275 μm × 90 μm rectangular cross-sections.

Thus, it has been shown here that SiO<sub>2</sub> glass fibers can in principal be produced by the extrusion and sintering route. However, a number of problems remain to be solved. While the drawing process will not impact the purity of the silica glass to a significant degree, the extrusion method involves considerable moving contact of silica powder with steel surfaces during mixing (mixer chamber and rotors) and extrusion (extruder barrel and dies). Undoubtedly some contamination of the fibers occurs as a result, and this can only be minimized by in future replacing all metallic contact surfaces with hard ceramics. Furthermore, the process needs to be developed further to permit the fabrication of distortion-free continuous fibers. The quality of the extrusion dies, i.e. corner sharpness and smoothness of the die land, must also be improved from the current state.

Despite these open issues, being able to produce fibers by the nanopowder extrusion route remains an attractive prospect. Regarding processing temperatures, the maximum temperature required for the extrusion and sintering approach is significantly lower than that required for drawing, in the present case 1100 °C instead of > 1600 °C, respectively. The main strength of the process, however, is that practically any material available in powder form, even those with extremely high melting and decomposition temperatures in ex-

cess of 2000 °C which cannot practically be drawn, can be formed into fibers with noncircular cross-sections.

\*

This paper is based in part on the diploma thesis entitled "Untersuchung zur Herstellung von SiO<sub>2</sub>-Glasfasern mit komplexer Geometrie" (Ilmenau Technical University, 2002) by J. Heiber from EMPA.

The authors thank all involved for their contributions to this work. Special thanks go to O. Burgold for preparing the SiO<sub>2</sub> preforms. Financial support was provided by the BBW (Office for Education and Science, Switzerland) under Project No. 00.0500 as part of the Disappearing Computer (DC) IST European Research Program (IST-200-25247).

## 5. References

- [1] Clemens, F., Wegmann, M., Mathewson, A. et al: Computing fibres: A novel fibre for intelligent fabrics? *Adv. Eng. Mater.* **5** (2003) no. 9, pp. 682–687.
- [2] Rabinovich, E.: Review: Preparation of glass by sintering. *J. Mater. Sci.* **20** (1985) pp. 4259–4297.
- [3] Woolley, F.: Melting/Finishing. In: *Engineered Materials Handbook*. Vol. 4: Ceramics and Glasses. Materials Park, OH: ASM International, 1991. Pp. 386–393.
- [4] Jansen, K.; Ulrich, R.: Drawing glass fibers with complex cross section. *J. Lightwave Technol.* **9** (1991) no. 1, pp. 2–6.
- [5] LaCourse, W. C.: Continuous filament fibres by the sol-gel process. In: *Sol-Gel Technology for Thin Films, Fibres, Preforms, Electronics, and Specialty Shapes*. Park Ridge, NJ: Noyes, 1988. Pp. 184–198.
- [6] Sakka, S.: Fibres from the sol-gel process. In: *Sol-Gel Technology for Thin Films, Fibres, Preforms, Electronics, and Specialty Shapes*. Park Ridge, NJ: Noyes, 1988. Pp. 140–161.
- [7] Papanikolaou, E.; Meerman, W.; Aerts, R. et al.: Preparation of ultra-pure silica glass from autoclave-dried gels. *J. Non-Cryst. Solids* **100** (1988) pp. 247–249.
- [8] Clasen, R.: Preparation and sintering of high-density green bodies to high-purity silica glasses. *J. Non-Cryst. Solids* **89** (1987) pp. 335–344.
- [9] Clasen, R.: Process and equipment for the fabrication of glass bodies by extrusion. *Europ. pat.* EP 0 200 243 B1. Applied for 21 March 1986; patent granted 30 May 1990.
- [10] Heiber, J.; Clemens, F.; Graule, T. et al.: Fabrication of SiO<sub>2</sub> glass fibres by thermoplastic extrusion. *Glass Sci. Technol.* **77** (2004) pp. 211–216.
- [11] Heiber, J.: *Untersuchung zur Herstellung von SiO<sub>2</sub>-Glasfasern mit komplexer Geometrie*. TU Ilmenau, Dipl. Ing. thesis 2002.
- [12] Tajima, K.; Tateda, M.; Ohashi, M.: Viscosity of GeO<sub>2</sub>-doped silica glasses. *J. Lightwave Technol.* **12** (1994) no. 3, pp. 411–414.
- [13] Clemens, F.; Wallquist, V.; Buchser, W.: Processing of silicon carbide fibers and microtools. *Subm. to Ceram. Int.* 2004.

■ E205N004

### Contact:

Dr. M. Wegmann  
EMPA Dübendorf  
Überlandstraße 129  
CH-8600 Dübendorf  
E-mail: markus.wegmann@empa.ch